J Neurol (2017) 264:2053–2067
DOI 10.1007/s00415-017-8547-3

REVIEW

Quantifying fat replacement of muscle by quantitative MRI in muscular dystrophy

Jedrzej Burakiewicz[1] · Christopher D. J. Sinclair[2,3] · Dirk Fischer[4,5] · Glenn A. Walter[6] · Hermien E. Kan[1] · Kieren G. Hollingsworth[7]

Received: 3 April 2017 / Revised: 12 June 2017 / Accepted: 13 June 2017 / Published online: 1 July 2017

Abstract The muscular dystrophies are rare orphan diseases, characterized by progressive muscle weakness: the most common and well known is Duchenne muscular dystrophy which affects young boys and progresses quickly during childhood. However, over 70 distinct variants have been identified to date, with different rates of progression, implications for morbidity, mortality, and quality of life. There are presently no curative therapies for these diseases, but a range of potential therapies are presently reaching the stage of multi-centre, multi-national first-in-man clinical trials. There is a need for sensitive, objective end-points to assess the efficacy of the proposed therapies. Present clinical measurements are often too dependent on patient effort or motivation, and lack sensitivity to small changes, or are invasive. Quantitative MRI to measure the fat replacement of skeletal muscle by either chemical shift imaging methods (Dixon or IDEAL) or spectroscopy has been demonstrated to provide such a sensitive, objective end-point in a number of studies. This review considers the importance of the outcome measures, discusses the considerations required to make robust measurements and appropriate quality assurance measures, and draws together the existing literature for cross-sectional and longitudinal cohort studies using these methods in muscular dystrophy.

Keywords Muscular dystrophy · MRI · Quantitative · Duchenne · Muscle · Clinical trial

✉ Kieren G. Hollingsworth
kieren.hollingsworth@newcastle.ac.uk

[1] Department of Radiology, C. J. Gorter Center for High Field MRI, Leiden University Medical Centre, Leiden, The Netherlands

[2] MRC Centre for Neuromuscular Diseases, UCL Institute of Neurology, London, UK

[3] Neuroradiological Academic Unit, UCL Institute of Neurology, London, UK

[4] Division of Neuropaediatrics, University of Basel Children's Hospital, Spitalstrasse 33, Postfach, Basel 4031, Switzerland

[5] Department of Neurology, University of Basel Hospital, Petersgraben 4, Basel 4031, Switzerland

[6] Department of Physiology and Functional Genomics, University of Florida, Gainesville, FL 32610, USA

[7] Newcastle Magnetic Resonance Centre, Institute of Cellular Medicine, Newcastle University, Newcastle-upon-Tyne, UK

Introduction: a motivation for quantifying muscle replacement by fat

All muscular dystrophies (MD) are rare orphan diseases, characterized by progressive muscle weakness resulting in functional disability. While the causes for muscle weakness vary between different MDs, they share common histological features, including fibrosis, muscle edema, and fat replacement of muscle tissue. More than 70 distinct variants have been identified, some becoming apparent in early childhood with rapid progression while others are not detected until adulthood with a much slower timescale of progression. Among the muscular dystrophies, Duchenne muscular dystrophy (DMD) is the most common form affecting 1 in 3500–6000 male births [1, 2], tending to show first symptoms at 3–5 years of age and rapid progression leading to loss of ambulation between 10 and 15 years. Deterioration of respiratory function and cardiomyopathy occur in DMD and in many other MDs.

Planning clinical trials of therapy in MDs is challenging for three reasons. First, the progression of the disease does not always follow a linear course when

physical abilities are measured. Longitudinal studies using clinical measurements in DMD show an improvement of gross and fine motor function up to the age of 7, a plateau phase up to the age of 10 followed by a phase of rapid decline during which free ambulation is lost [3, 4]. Second, recruitment in rare disease cohorts for large clinical trials is difficult. Third, clinical assessment is dependent on cooperation (especially in children) and the measurements required differ between ambulant and non-ambulant patients.

Therefore, it is essential to have outcome measures that are less dependent on patient cooperation and motivation while being sufficiently sensitive to measure treatment effects even in small and highly heterogeneous patient populations. Quantitative muscle MRI (qMRI) can provide such an outcome measure, as it is non-invasive and can generate a wide range of imaging contrasts over large volumes of muscle. As such, it can visualize and quantify the major hallmarks of muscle degeneration in MDs: muscle hypertrophy and atrophy, muscle edema and inflammation, and the replacement of muscle tissue by fat tissue. Histologically, the content of the muscle fibres is progressively replaced by lipid, resulting in a fatty tissue. On MRI, the overall outline, shape, structure, and appearance of the muscle groups are often preserved despite the extensive fatty tissue content. In contrast to functional scores obtained by physical assessment, qMRI is less biased by patients or observers. Excellent reproducibility of qMRI has been demonstrated in healthy volunteers as well as in patients [5, 6]. In particular, qMRI of fat replacement has the potential to be very valuable as an outcome measure in clinical trials as it has been shown to be more sensitive than clinical evaluation in detecting disease progression [7–12] and effect sizes of fat replacement measured by qMRI are much greater than those of commonly used clinical scores [10, 13]. Thus, when using qMRI of fat replacement as an end-point to demonstrate the effectiveness of a putative novel treatment, the number of patients required is markedly reduced [9, 10]. Although invasive muscle biopsy is sometimes undertaken (often to determine membrane protein expression) and fat content could be estimated from it, it is an unreliable method of measuring fat content due to the small sample volume, the heterogeneous nature of the fat replacement across muscle groups, and the limitations on repeating biopsy in longitudinal studies.

In this review, we review the MRI sequences used to quantify fat replacement of skeletal muscle by imaging and detail the important factors that need to be taken into account to produce accurate results ("Quantitative fat fraction imaging measurements: how is it done?"), compare these with magnetic resonance spectroscopy methods ("T2-corrected spectroscopy to measure muscle fat content"), and provide a survey of longitudinal and cross-sectional studies of muscular dystrophy which have employed variants of these methods ("Studies which have used quantitative fat fraction measurements in muscular dystrophy"). We then consider the quality assurance required for using these methods ("Quality assurance") and practical considerations for patient positioning, slice prescription, and data analysis ("Patient placement, acquisition time and scan acceleration, practical issues and segmentation"). Most MR vendors have developed products for measuring liver steatosis and we discuss the necessary considerations for using these in skeletal muscle ("Vendor implementations of quantitative protocols to measure PDFF").

Quantitative fat fraction imaging measurements: how is it done?

T1-weighted imaging as fat quantification technique

While T1-weighted MRI is commonly used in routine diagnostic procedures to assess muscle involvement, T1-weighted imaging has several disadvantages when it is used to measure fat replacement. First, the signal intensity does not directly quantify changes in muscle fat content and needs to be referenced, e.g., to the subjects' bone marrow intensity of the same image section and expressed as a percentage of the bone marrow signal intensity [14]. Second, quantifying muscle signal intensity with T1-weighted imaging is subject to B_1 and B_0 inhomogeneities [14], as shown in Fig. 1. Finally, T1-weighted imaging is less sensitive than quantitative MRI at detecting fat changes in muscle of patients with MD [7, 11–13], as described in the next section. Overall, we do not recommend using T1-weighted imaging as a quantitative measure. In the following sections, we instead describe the principles of quantitatively measuring fat using chemical shift imaging techniques.

Principles of fat fraction measurement using chemical shift differences

The protons within water and lipids resonate at slightly different frequencies. For example, the CH_2 groups in the fatty acid chains resonate at a lower frequency than water. In a gradient echo scan, this means that though the CH_2 and water spins start off in phase immediately after the initial excitation pulse, like two men running on a circular racetrack at different speeds, there is an echo time when the signals from water and CH_2 are on the opposite side of the racetrack, that is to say 180° out of phase and their signals will cancel. By acquiring an image after twice this echo time has elapsed, the water and CH_2 would be back in phase, and their signals will add (Fig. 2). In principle, by

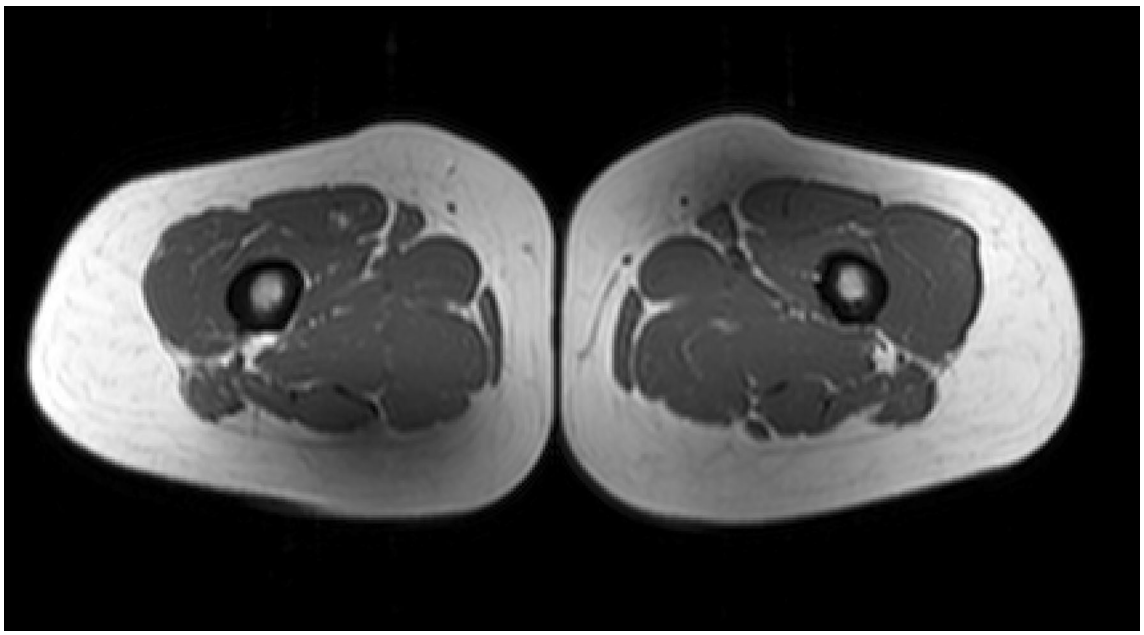

Fig. 1 T1-weighted image of dystrophic thigh muscle. The widely varying signal intensity in the uniform subcutaneous fat demonstrates the B_1 inhomogeneity across the leg at 3.0 T which inhibits the ability of T1-weighted images to monitor disease progression

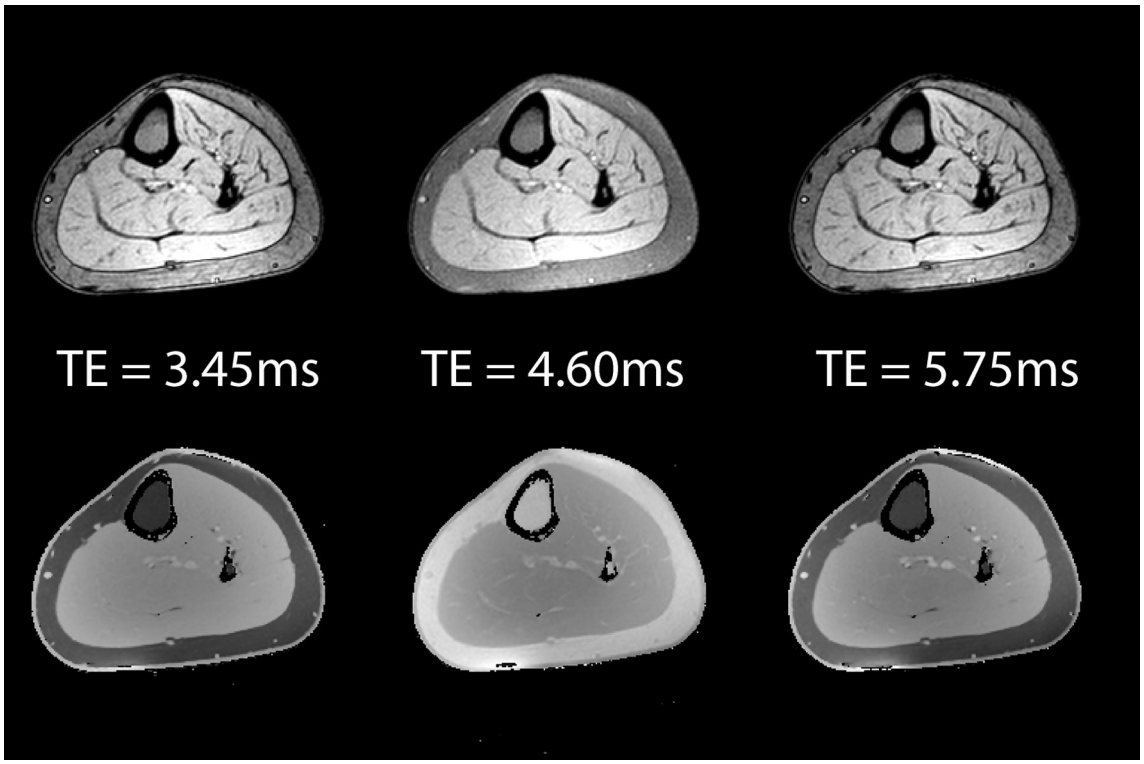

Fig. 2 Cross-section through healthy lower leg muscle with a gradient echo sequence using (*left*) out of phase (TE = 3.45 ms), (*middle*) in phase (TE = 4.6 ms), and (*right*) out of phase (TE = 5.75 ms) echo times. The *top row* shows the magnitude signal, while the *bottom shows* the phase. Note the cancellation of the magnitude signal at water–fat boundaries in the out of phase images

acquiring images at the two time points described and by adding and subtracting the signal, we can produce images purely of fat and of water (Fig. 3). The respective fat and water signals can then be used to calculate the fat fraction, expressed as the fraction of fat signal in the total signal in each voxel (Fig. 4):

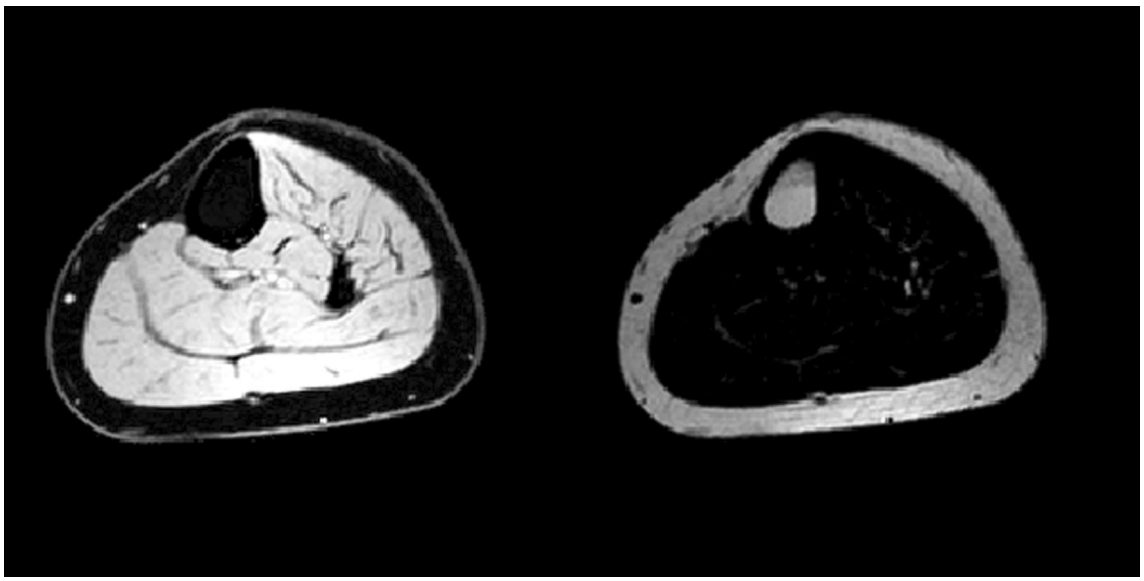

Fig. 3 Use of a mathematical model enables the signal from the water components and the fat components to be separated, though these images still contain B_1 inhomogeneity

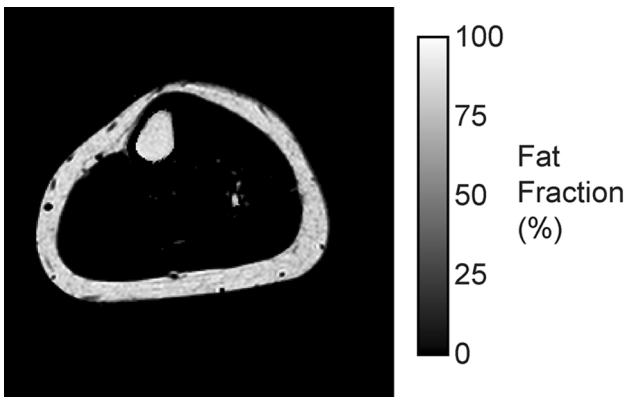

Fig. 4 If we calculate the percentage of fat signal in the total MR signal, then the background inhomogeneity disappears and we are left with a map of fat fraction from 0 to 100% which is comparable between scan sessions and individuals

$$\eta = \frac{S_F}{S_F + S_W}$$

where η is the fat fraction, and S_F and S_W are, respectively, fat and water signals [15].

One major limitation of this simple, so-called, two point Dixon approach [16] is that it assumes that the magnetic field is homogeneous everywhere, which is generally not true. However, this complication can be accommodated by acquiring a third echo [17], giving rise to the so-called three-point Dixon method. Although the original papers describing this approach envisaged using purely in phase and out of phase echo times, this is not mandatory and the fat and water signals can be separated using other echo times with a more general signal model [18].

Most work in neuromuscular diseases has been performed with either 2 or 3 gradient echoes, sometimes collected within a single TR (which is faster) or sometimes in separate TRs. More than three echoes can be collected for better signal-to-noise ratio and for improved precision of the fat fraction measurement (see "Advanced: choosing echo times and signal efficiency").

What to look out for when processing quantitative fat imaging

While calculating the fat fraction from the water and fat images may seem straightforward, there are several confounding factors to consider. If the measure is going to be used as a biomarker, particularly in multi-centre studies, it should be accurate, reproducible, and independent of the precise scan parameters used. For this reason, the proton density fat fraction (PDFF) (which has been previously recommended for liver studies) is a suitable measure. PDFF is the ratio of the density of mobile triglyceride protons to the total density of mobile protons that are MR visible [15, 19, 20]. Note that the PDFF is not an absolute concentration of fat, but a relative one. In the presence of edema and fibrosis, the measured water signal is not the same as the absolute water content of the voxel. While it can be shown that the PDFF is linearly correlated to the mass fat fraction, the correlation coefficient strongly

Table 1 Confounders to fat fraction analysis

Confounding factor	Origin	Effect if ignored	Solution
Acquisition sequence is T1-weighted	Water and fat have very different T1 relaxation times in muscle	The reported fat fraction is artificially high	(a) Avoid T1-weighting using long TR and low flip angle [64] (b) Post-processing correction with pre-calibrated data [15, 65]
Fat spectrum is not fully represented by CH_2 alone $\sim$30% of the proton signal lies away from the CH_2 peak – Fig. 5 [12, 62, 66]	The lipid resonance has multiple resonant frequencies other than the CH_2 peak (Fig. 5)	The reported fat fraction is artificially low	Use a fat–water separation model that permits a multi-spectral model, containing typically 6 or 9 spectral components [67, 68]
Not accounting for T2* relaxation	The effective $T2^*$ produces weighting in a series of gradient echo images with varying TE. $T2^*$ varies with muscle involvement	Low fat fractions have positive bias, uncertainty in PDFF at low fat fraction [43]	Use a fat–water separation model that allows a single $T2^*$ component to be specified [43]
Biased fat fractions near PDFF $\approx$ 0% and 100%	Noise bias caused by magnitude correction	Fat fractions positively or negatively biased	Calculate the PDFF using a noise bias correction method [64]
Phase inaccuracy	Bipolar readouts, eddy currents, diffusion gradients [15, 20, 64, 69, 70]	Artefacts in the fat fraction map	(a) Use sequences with monopolar readouts (b) Correct modelling for eddy currents or bipolar readouts

depends on the tissue studied; PDFF can serve, however, as an independent biomarker in its own right [19].

There are several major confounding factors that need to be accounted for and mitigated: Table 1 lists the main factors, their effects, and suggested solutions. In summary, a properly implemented fat–water separation method with sufficient long TR and low FA to minimise T1-weighting, three or more echoes, using multi-spectral modelling of fat and T2* correction can yield a quantitative value that can be compared both longitudinally and cross-sectionally between centres subject to appropriate quality assurance procedures ("Quality assurance").

Advanced: choosing echo times and signal efficiency

The echo spacing for the traditional gradient echo in and out of phase images can be worked out as follows: with a 435 Hz difference at 3.0 T, the signals are in phase 435 times per second, so after the start, they are in phase again after 1/435 s = 2.3 ms; thus, they will be out of phase for the first time at 1.15 ms and every 2.3 ms after that. The signal-to-noise efficiency of Dixon imaging can be increased by varying the echo spacing, so that the intervals no longer correspond to the in and out of phase echo times. Reeder and colleagues introduced this concept by calculating the echo intervals that maximise the effective signal to noise across the range of fat fractions for a multi-echo acquisition [18, 21]. When combined with an iterative algorithm for the fat–water separation, this approach is known by the acronym IDEAL (iterative decomposition of water and fat with echo asymmetry and least-squares estimation). However, the purpose remains the same as the 2 and 3 point Dixon techniques.

Measuring T2 and PDFF with the same sequence

The majority of 2 and 3-point Dixon applications in skeletal muscle have used gradient echo readouts. However, spin-echo (SE) and fast spin-echo (FSE) may also be used as originally proposed by Glover and Schneider [17]. One possible factor contributing to limited use of spin-echo Dixon techniques is increased scan times due to prolongation of the repetition time for multi-slice imaging [22].

Often, PDFF and the T2 relaxation time of water, a surrogate for inflammation and edema, are measured using two different sequences. The efficiency of the scan can be improved by measuring them using the same sequence. IDEAL fat–water separation has also been combined with a CPMG spin-echo train in the so-called IDEAL-CPMG sequence [23]. Although IDEAL-CPMG is thus far not widely available, this approach enables independent measurements of the T2-relaxation times of the separated fat and water components in skeletal muscle, an important capability in conditions where water- and fat-based pathologies may exist simultaneously [24, 25].

T2-corrected spectroscopy to measure muscle fat content

Traditionally, spectroscopic methods have been used to determine changes in lipid content (both intramyocellular (IMCL) and extramyocellular (EMCL) lipids), lipid saturation, and major muscle metabolites including trimethyl ammonium compounds (e.g., choline and carnitine), creatine, carnosine, acylcarnitines, and lactate [26]. Proton

MRS can also be used to determine absolute tissue water and lipid content with high accuracy and reproducibility using both internal and external referencing methods [27, 28]. In the presence of fibrosis and/or edema, commonly found in muscular dystrophies, absolute water content can only be obtained using an external reference method. However, this is currently not commonly applied. As described above for the imaging methods, corrections for T2 and T1 relaxation need to be applied for the individual metabolites to calculate a PDFF. In addition, the relative contribution of each resonance to the overall lipid content signal (Fig. 5) needs to be determined. MRS determined fat fractions have become the standard against which to validate PDFF calculations based on imaging techniques [29–31]. An advantage of MRS is that the fat fraction measurement is made directly from the spectral peaks representing the lipids present. In imaging methods, a fixed lipid spectral model of lipid is necessary. Therefore, information can sometimes be obtained about triglyceride properties with MRS, including the level of carbon chain unsaturation. Whereas high-resolution MR spectroscopy will resolve all the major lipid resonances, at clinical field strengths, individual lipid resonances may need to be deconvolved using a number of different spectral processing techniques [32].

Whereas accelerated multi-voxel spectroscopic imaging techniques have been developed [33] and implemented in muscle [34], the spatial resolution is less than that obtained with MRI and 3D coverage has been limited by long acquisition times. Signal bleeding from neighboring voxels can influence accuracy. Hence, most MRS measures of PDFF have been based on targeted, single voxel spectroscopy [10, 35–38]. A disadvantage of this localization method is the relatively large voxel size; voxels are typically an order of magnitude bigger in size than MRI, and range from 5 to 20 ml. While this is beneficial from a signal-to-noise ratio (SNR) perspective and enhances greater detection sensitivity to low fat concentrations, it requires accurate voxel placement and extensive operator training. In practice, it is feasible to obtain MR spectra of only a couple of selected muscles within a single examination.

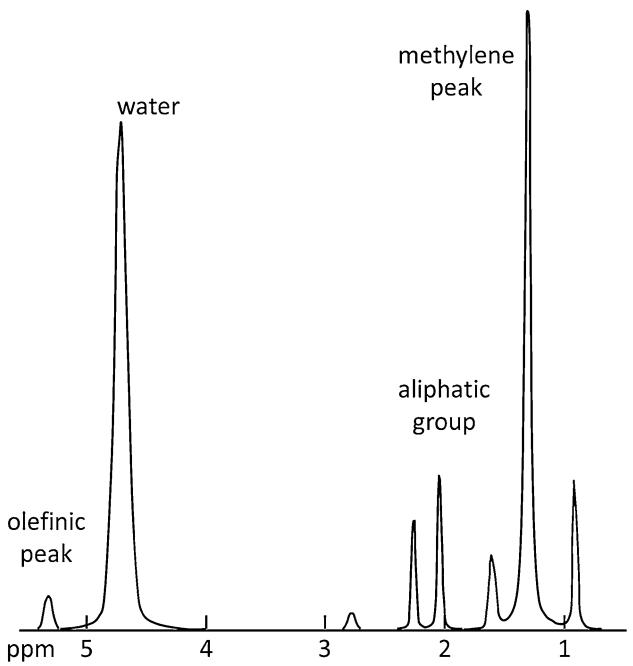

Fig. 5 Typical water–fat spectrum based on ref 68. Fat signal is often modelled on one off-resonant frequency (1.3 ppm); however, this is not accurate, since up to 30% of fat signal may lie at different locations. For true quantitative measurements, the entire fat spectrum should be accounted for

Studies which have used quantitative fat fraction measurements in muscular dystrophy

The first study using the Dixon approach to examine the fat content of dystrophic muscle in humans was published in 2008 (Table 2). In the period since then, and particularly in the last 4 years, qMRI methods to quantify fat replacement have been performed in many neuromuscular diseases. It is arguable that this work has been stimulated by the prospect of first-in-human trials in some conditions, particularly DMD. In this section and the adjoining tables, we summarise the studies that have been undertaken.

In the tables, the studies have been categorised in three groups. First, those studies which have been undertaken on a cross-sectional cohort of a particular form of muscular dystrophy are shown in Table 2. These studies have typically been performed to determine the pattern of fat replacement within a cohort and to describe cross-sectional changes with increasing age. The main focus of these studies has been on the dystrophinopathies. In general, the involvement pattern varies considerably between different diseases, where one muscle can be affected early in one disease and be spared until late in the disease process in another. A typical example is the clear involvement of the soleus muscle in the calf of OPMD patients [5], while this muscle is involved only after the tibialis anterior and peroneal muscles become affected in DMD [39]. In addition to differences between diseases, within a particular disease with the same underlying genetic defect, the fatty replacement of individual muscle groups can vary widely, as demonstrated in a multi-national LGMD2I cross-sectional study [40]. Often, the fat fraction measurements from individual muscle groups have been correlated against physical function tests. In general, fat fractions correlate well with functional tests. However, especially in DMD and BMD, it has been shown that contractile

Table 2 Cross-sectional cohort studies

Study	Field (T)	Population	No. of patients	Method	Multi-spectral model?	T2* corrected?	Correlations?
Fischmann et al. [5]	1.5	OPMD	8	2 point	No	No	Function
Fischmann et al. [71]	3.0	DMD	20	2 point	No	No	Function
Forbes et al. [37]	3.0	DMD	123	MRS	n/a	n/a	N/a
Gaeta et al. [72]	1.5	DMD	20	2 point	No	No	Function
Hooijmans et al. [46]	3.0	DMD	18	3 point	Yes	No	T2,^{31}P MRS
Hooijmans et al. 2017 [73]	3.0	DMD	22	3 point	Yes	No	Modelling of non-uniformity of fat replacement in proximodistal axis
Horvath et al. [74]	3.0	LOPD	7	2 point	Yes	Yes	Function
Lokken et al. [41]	3.0	BMD	14	2 point	n/k	n/k	Muscle strength to cross-sectional area
		LGMD2I	11				
Mankodi et al. [24]	3.0	DMD	13	3 point IDEAL-CPMG	Yes	n/a	Use of IDEAL-CPMG sequence to measure fat fraction and T2 in Duchenne. Small longitudinal follow-up group
van den Bergen et al. 2014 [75]	3.0	BMD	9	3 point	Yes	No, global T2 correction	Dystrophin levels
Willcocks et al. [52]	3.0	DMD	22	MRS and 3 point	Yes	Yes	Performance of upper limb test, grip strength
Willis et al. [40]	3.0	LGMD2I	38	3 point	No	No	Function
Wokke et al. [76]	3.0	BMD	25	3 point	Yes	No, global T2 correction	Function and^{31}P MRS
Wokke et al. [39]	3.0	DMD	16	3 point	Yes	No, global T2 correction	Function
Wren et al. [77]	1.5	DMD	9	3 point	No	No	Function

n/a not applicable, *n/k* not known from manuscript, *OPMD* oculopharyngeal muscular dystrophy, *DMD* Duchenne muscular dystrophy, *LGMD2I* limb girdle muscular dystrophy 2I, *BMD* Becker muscular dystrophy, *LOPD* late-onset Pompe's disease (glycogen storage disease type II)

properties are disrupted, because specific force is reduced [39, 41]. This type of analysis is performed using Dixon imaging to generate a maximal contractile cross-sectional area and then comparing this to muscle strength measurements.

To prepare qMRI end-points for clinical trials, it is important to know in which muscle groups fatty replacement will progress in the absence of remedial treatment, as rates of progression vary between different muscle groups and over time. The most suitable muscle group to follow will depend on several factors, including age, type of disease, and mechanism of action of the drug. For instance, the efficacy of a drug that is thought to prevent a further increase in fat replacement would be most suitable to test in a muscle and age group where there is a clear increase in fat replacement over time. This muscle group will then have the highest standardized response mean. In DMD, for instance, it has been suggested that between the ages of 9 and 11 years, the vastus lateralis has the highest standardized response mean [10]. On the other hand, a drug that aims to increase muscle mass can also be evaluated in a muscle that does not show fat replacement yet, merely by assessing at the contractile volume. Table 3 outlines the longitudinal studies that have been performed in different

Table 3 Studies with longitudinal data measuring fat fraction

Study	Field (T)	Population	No of patients	Method	Multi-spectral model?	T2* corrected?	Longitudinal interval(s)	Correlations
Andersen et al. [78]	3.0	FSHD	45	2 point	n/k	n/k	1 year	Function
Arpan et al. [35]	3.0	DMD	15	MRS	n/a	n/a	3 months, 6 months, 1 year	Corticosteroid use, function
Bonati et al. [79]	3.0	DMD	20	2 point	No	No	1 year	Motor function
Bonati et al. [80]	3.0	BMD	3	2 point	No	No	1 year	
Bonati et al. [81]	3.0	SMA	18	2 point and 6 point	No Yes	No Yes	3 months, 6 months, 1 year	Function, molecular biomarkers
Carlier et al. [42]	3.0	LOPD	23	3 point	n/k	n/k	1 year	Enzyme replacement therapy
Fischmann et al. [7]	1.5	OPMD	5	2 point	No	No	13 months	Function
Hogrel et al. [8][a]	3.0	DMD	25	3 point	n/k	n/k	1 year	Function
Morrow et al. [9]	3.0	CMT1A IBM	20 20	3 point	n/k	n/k	1 year	Function
Ricotti et al. [44][a]	3.0	DMD	15	3 point	No	No	3 months, 6 months, 1 year	Performance of upper limb, pinch strength
Wary et al. [54][a]	3.0	DMD	24 (9)	3 point	n/k	n/k	1 year	Ambulation
Willcocks et al. [10]	3.0	DMD	109	MRS	n/a	n/a	3 months ($n = 11$) 6 months ($n = 15$) 1 year	Function
Willis et al. [11]	3.0	LGMD2I	32	3 point	No	No	1 year	Function, FVC

n/a not applicable, *n/k* not known from manuscript, *FSHD* facioscapulohumeral muscular dystrophy, *OPMD* oculopharyngeal muscular dystrophy, *DMD* Duchenne muscular dystrophy, *LGMD2I* limb girdle muscular dystrophy 2I, *BMD* Becker muscular dystrophy, *LOPD* late-onset Pompe's disease (glycogen storage disease type II), *CMT1A* Charcot-Marie-Tooth disease 1A, *IBM* inclusion body myositis, *SMA* spinal muscular atrophy

[a] Study of the upper limb

muscular dystrophies to measure the rates of progression. Figure 6 shows two examples of fat fraction progression across 1 year in a slow-progressing muscular dystrophy, LGMD2I [11], and one in the more rapidly progressing DMD. Most of these studies have examined the natural history of different diseases, though Arpan et al. 2014 considered the effects of corticosteroid initiation in DMD boys [35] and Carlier et al. 2015 [42] examined the effect of enzyme replacement therapy in late-onset Pompe's disease. Commonly, these longitudinal studies contrast the increase in muscle fat fraction revealed by qMRI and disease progression demonstrated by the standard physical function tests that are routinely used in clinical care and clinical trials. These studies have demonstrated the enhanced sensitivity of qMRI compared to the existing measurements in both the legs [9–11, 24, 43] and the arms [8, 44].

Finally, some studies on neuromuscular disease have been performed to investigate new MR methods in these patients, but contain valuable information about patient cohorts (Table 4). These include quality assurance and reproducibility studies [25, 38], work to accelerate image acquisition [43, 45], and correlations between MRI and MRS methods [38, 46].

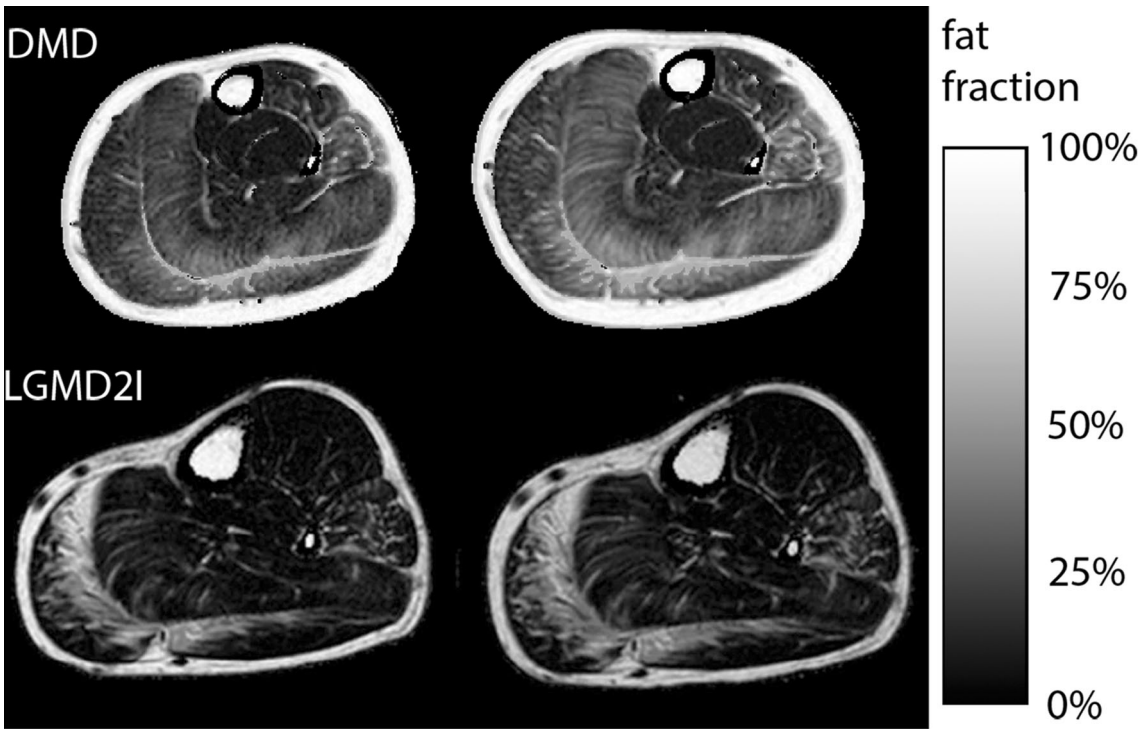

Fig. 6 Example of using PDFF maps to assess progression at baseline (*left*) and 12 months later (*right*) in the lower leg of a patient with limb girdle muscular dystrophy 2I (*bottom*) and Duchenne muscular dystrophy (*top*). Progression in 1 year is generally much more rapid in DMD compared to LGMD2I: fat fraction changes measured included the soleus (21–28% in DMD, 8–13% in LGMD2I), tibialis anterior (12–16% in DMD, no change at 6% in LGMD2I), lateral gastrocnemius (21–29% in DMD, 20–24% in LGMD2I), medial gastrocnemius (15–20% in DMD, 29–49% in LGMD2I), and the peroneus (28–36% in DMD, 18–26% in LGMD2I)

Quality assurance

PDFF as determined by MRI is a derived value based on multiple analytical steps (see "Quantitative fat fraction imaging measurements: how is it done?"). In the pure research environment, each of these steps may be continually monitored and quality controlled using validation data test sets and tissue phantoms. This might not always be possible in the purely clinical environment in which fat/water maps are provided solely as derived DICOM images generated by vendor specific software. As outlined in "What to look out for when processing quantitative fat imaging" and Table 1, techniques for separating fat and water have evolved to include more complex models for lipids as well as to take into T2* relaxation into account. Therefore, it is essential to continually monitor these derived values using known standards to address both the accuracy and precision of the PDFF measurements. Whereas monitoring the precision of the PDFF within a single site may be sufficient, clearly a high level of accuracy is essential for continuity between sites and studies in longitudinal, multi-site trials. During a quality control and validation stage, accuracy and precision can be readily tracked and documented using a combination of MRS and MRI methods on both phantoms and human test subjects. Some clinical trials that use MRI as an end-point now demand that a calibrated test object is scanned before or after every subject visit to monitor system and measurement stability.

Whereas there is currently no standard for quality control measures for PDFF MRI determination, a number of viable options exist.

Intralipid-based phantoms

Similar to common T1 and T2 calibration phantoms, vials containing different PDFF values can be made. A simple phantom can be constructed from a copper sulphate solution, pure soybean oil, and commercially available Intralipid (Registered-Baxter Healthcare Corporation) emulsions at different concentrations (available at 10 and 20%). Analysis of the images will yield a reference curve that can be matched to single MRS acquisitions to determine the linearity and agreement between MRS and MRI PDFF. This tissue phantom is easy to create and allows for testing changes in T1 and T2* in the aqueous solutions.

Table 4 Studies principally concerning MR methodology which contain patient populations

Study	Field (T)	Population	No. of patients	Method	Multi-spectral model?	T2* corrected?	Study topic
Azzabou et al. [82]	3.0	Multiple	48	3 point	no, post hoc adjustment	no	Validation of a three exponential model for fitting multi-echo T2 data
Forbes et al. [36]	3.0	DMD	30	MRS	n/a	n/a	Reproducibility study
Gloor et al. [13]	1.5	OPMD	8	2 point	No	No	Comparison of fat imaging techniques
Hollingsworth et al. [45]	3.0	BMD	8	3 point	Yes	No	Scan acceleration by compressed sensing techniques
Hooijmans et al. [83]	3.0	DMD	24	3 point	No	No	Diffusion tensor imaging
Lareau-Trudel et al. [56]	1.5	FSHD	35	T1-weighted	No	No	Automated evaluation
Loughran et al. [43]	3.0	BMD	8	3 point, 6 point	Yes	Yes	Scan acceleration by compressed sensing techniques, role of T2* correction
Mankodi et al. [24]	3.0	DMD	13	3 point IDEAL-CPMG	Yes	n/a	Use of IDEAL-CPMG sequence to measure fat fraction and T2 in Duchenne. Small longitudinal follow-up group
Marty et al. [84]	3.0	Mixed	22	3 point	No, post hoc adjustment	No	Validation of extended phase graph method for fitting multi-echo T2 data
Ponrartana et al. [85]	3.0	DMD	13	6 point	Yes	Yes	Diffusion tensor imaging
Sinclair et al. [25]	3.0	HypoPP	12	3 point IDEAL CPMG	Yes	n/a	Stability and sensitivity of IDEAL-CPMG sequence to measure fat fraction and T_2
Triplett et al. [38]	3.0	DMD[a], COL6[b]	71[a] 16[b]	3 point, MRS	Yes	No	Correlation of MRI and MRS methods
Wokke et al. [12]	3.0	DMD	13	3 point	Yes	No, global T2 correction	Comparison of multi-spectral models and qualitative grading systems

n/a not applicable, *n/k* not known from manuscript, *OPMD* oculopharyngeal muscular dystrophy, *DMD* Duchenne muscular dystrophy, *BMD* Becker muscular dystrophy, *LOPD* late-onset Pompe's disease (glycogen storage disease type II), *COL6* collagen VI deficiency, *HypoPP* hypokalemic periodic paralysis, *FSHD* facioscapulohumeral muscular dystrophy

Fat/water container

For example, a sample bottle in which two layers of fluid have been introduced, water and oil, to form two immiscible layers, with no emulsified droplets at the boundary. For 2D acquisitions, images can be acquired, such that the slice thickness progressively moves through the water/fat interface, by an increment of 0.5–1 mm each time [47]. This will build up a series of images where the composition of the slice changes from 0% fat to 100% in known increments. Another option is to use an angled slice through the fat/water interface; in this way, a gradient of PDFF can be created from 0 to 100% [38]. Analysis of these images can yield a reference curve that can be directly matched to single voxel MRS acquisitions to determine the linearity and agreement between MRS and MRI determined PDFF. This phantom does not allow testing of reconstruction algorithms that take into account differences in T1 and T2* on the derived PDFFs.

Customized water–fat emulsions and agar gels

Water and fat emulsions for PDFF calibration have been created from soya and carrageenan [48] or peanut oil and 2% agar [49]. To achieve homogenous mixing and stability, it is necessary to add surfactant and sodium azide to the emulsion. This phantom has the advantage that different concentrations of superparamagnetic iron oxide can be mixed in to provide T2* weighting at the different fat fractions ranging from 0 to 100%. Moreover, this phantom has the advantage that variable amounts of heavy water (D_2O) can be used as the solvent to simulate decreased H_2O proton density observed on the calculated PDFF [50]. Similar to above, accuracy and precision can be determined by determining the relationship between MRS and MRI derived PDFFs.

Patient placement, acquisition time and scan acceleration, practical issues and segmentation

For leg imaging, the preferred positioning is feet-first supine, with the legs stretched, the patella facing upward, and the ankles in the neutral position (i.e., minimal exo or endorotation). To enhance comfort, a small pillow can be placed under the knees, but the standard leg rest delivered with many scanners will not accommodate this, and the sides of the ankles can be supported with sandbags to prevent unintended movements. In patients with contractures positioning with stretched legs and neutral ankles is not always feasible, and care should be taken to provide optimal support for comfort. Positioning of the upper limb is more challenging, as scan quality is severely reduced at the side of the magnet bore. Experience with scanning of this body part is limited [8, 44, 51, 52], but it will become more common with the need to develop outcome measures for non-ambulant patients. The so-called 'superman' position [53] is likely impossible for patients with MDs, and hence, optimal positioning will either be (a) in the fetal position, (b) supine with the upper limb along the trunk, while the trunk is as far off-centre as possible [8, 44, 52, 54], or (c) supine with a dedicated arm rest placed over the abdomen of the patient: all published studies in DMD have so far selected the second option.

Imaging can be performed in 2D or 3D, with slices in the transverse plane perpendicular to the bone to facilitate analysis. The location of the slice stack should be recorded precisely to enable longitudinal measurements, for instance at a fixed distance from a bony landmark, such as the tibial plateau or the patella. Landmarking can either be done during the imaging session using a scout image [5] or prior to the scanning session by placing a fish oil capsule on the skin at a pre-defined distance from surface anatomy landmarks like the iliac crest [55]. Receiver coils can either be array coils for wide coverage of the lower limb or local surface coils. The latter may be more convenient for imaging the upper limb and for patients with contractures.

As fat replacement of muscle tissue can be non-uniform along the muscle length [51], it is important that the slice stack covers as much of the muscle as possible. Commonly, this is achieved by selecting a field of view from joint to joint, i.e., malleolus to patella for the leg, and patella to iliac crest for the thigh. Slice thickness is usually between 2 and 10 mm with a 0–5 mm gap, resulting in 10–50 slices per body part. This poses a significant burden in terms of data processing as traditionally, data are being processed by outlining every single muscle in a pre-defined number of slices by a trained operator—which is a labour intensive process. In the last decade, several techniques have been developed that can quantify total adipose tissue volume and total muscle volume based on either T1 weighted or Dixon images [52, 56–58]. In these approaches, the total muscle volume of an entire slice stack can automatically be segmented, thereby severely reducing the processing time. Unfortunately, severe fatty replacement is still a problem, as it is difficult to separate fat replacement from subcutaneous fat, and hence, user input is required to solve this [56, 59]. More importantly, as fatty replacement occurs in a muscle specific way, it is preferable to obtain information of each muscle separately instead of the entire muscle volume—and this is not possible using this methodology. While, semi-automatic approaches have been developed that can segment individual muscles [60, 61], these have not been applied in NMDs yet. In the absence of such an approach, segmentation is unfortunately still often performed manually and the field is in dire need of adequate approaches to solve this.

Depending on the choice of repetition time and number of signal averages used, a common Dixon acquisition of the entire upper leg can take 3–5 min. Using scan acceleration techniques, acquisition time can be reduced dramatically to about 1 min [43, 45]. However, these techniques are not yet standard on clinical systems.

Vendor implementations of quantitative protocols to measure PDFF

The basic types of multi-echo acquisition sequences described in "Quantitative fat fraction imaging measurements: how is it done?" can be achieved by most clinical MRI scanners in skeletal muscle, even where the echoes have to be collected in separate acquisitions. Historically, it has not been possible to buy directly from the vendor an integrated system that will both perform the data acquisition and reconstruct the proton density fat fraction images at the time of acquisition. Most of the studies described in "Studies which have used quantitative fat fraction measurements in muscular dystrophy" have extracted the complex image data from the scanner and applied custom algorithms, such as those described in [15, 17, 62] to separate the fat and water and produce fat fraction images. Of particular note was the ISMRM Workshop on Water–fat separation, which collated examples of MATLAB code which can achieve this task and have been made available [15].

Of course, the methods for measuring fat fraction have also found extensive use in the measurement of hepatic steatosis in type 2 diabetes and non-alcoholic fatty liver disease [63]. Given the size of these markets, the main MRI vendors have now released products, usually sold as optional upgrades to the base scanner hardware, which claim to reliably measure hepatic steatosis: IDEAL-IQ

(GE), mDixon Quant (Philips), and LiverLab (Siemens). However, it is important to note that these products and their optimised settings have not been validated in skeletal muscle and it should not be assumed that they will automatically give acceptable answers outside of their intended terms of use. The same quality assurance procedures outlined in "Quality assurance" should be adopted and consideration should also be given to the effect of a change of vendor software during the course of a longitudinal study.

Summary

Characterising rare muscle diseases with qMRI is an important task, because these techniques may be substantially more responsive than the existing clinical measures of function currently used as end-points in clinical trials [9–11]. However, there are various qMRI approaches available that are influenced by details of acquisition and reconstruction, and this should be taken into consideration when comparing results from different centres. In this paper, we have given a conceptual and practical introduction to Dixon fat fraction imaging and MRS, drawing attention to the advantages and potential confounding factors of each. The authors believe that fat fraction imaging and MRS will both have an important role to play in future scientific and therapeutic studies, with quantitative MRI methods more familiar to operators in most institutions. Regardless of the method used, adequate operator training, qualification, and quality assurance processes will be needed over and above those used for standard radiological imaging. This will demand specialist input to co-ordinate and oversee clinical trials involving quantitative MRI. Given the low prevalence of many of the muscular dystrophies, high quality data may demand that patients travel to a smaller number of centres specialising in quantitative MRI. Many new clinical trials for DMD now require quantitative MRI in at least a subset of patients.

Practical considerations for quality assurance, patient positioning, slice prescription, and the available vendor systems were introduced. By summarising the available literature describing the application of Dixon-based fat fraction imaging in muscle dystrophies, we hope to highlight the power and promise of these techniques, while emphasising that a pragmatic consideration of the limitations is essential to maximise the potential advantages that fat fraction imaging confers on longitudinal clinical trials in this important class of diseases.

The authors would suggest that, with the increasing availability of quantitative MRI methods on modern scanners, and the increasing bodies of longitudinal literature identifying target muscle groups to study in therapeutic interventions, the quantitative MRI methods are reaching maturity and will have a critical and central role to play and end-points in future therapeutic trials.

Acknowledgements This publication is supported by the European Union COST (Co-operation in Science and Technology) action BM1304, MYO-MRI (http://myo-mri.eu), which supports international collaboration on "Applications of MR imaging and spectroscopy techniques in neuromuscular disease: collaboration on outcome measures and pattern recognition for diagnostics and therapy development".

Compliance with ethical standards

Conflicts of interest JB reports grant support from the European Union (FP-7-HEALTH-2013-INNOVATION-1, 602485). CDJS declares no conflicts of interest. HEK reports grants from ZonMW, AFM, Duchenne Parent Project, the European Union (FP-7-HEALTH-2013-INNOVATION-1, 602485), and Gratama Stichting, consultancy for BioMarin and aTyr Pharma and trial support from ImagingDMD-UF outside the submitted work. All reimbursements were received by the LUMC; no personal benefits were received. DF declares no conflicts of interest. GAW has received Grant funding from the National Institutes of Health, Department of Defense, Muscular Dystrophy Association, Sarepta Therapeutics and Catabasis Pharmaceuticals. KGH reports grants from the United Kingdom Medical Research Council, Diabetes UK, the European Union (H2020, 667078) and the Newcastle Healthcare Charity, consultancy for Summit pharmaceuticals and trial support from ImagingDMD-UF outside the submitted work. All reimbursements were received by Newcastle University; no personal benefits were received.

References

1. Ellis JA, Vroom E, Muntoni F (2013) 195th ENMC international workshop: newborn screening for Duchenne muscular dystrophy 14–16th December, 2012, Naarden, The Netherlands. Neuromuscul Disord 23(8):682–689. doi:10.1016/j.nmd.2013.05.008
2. Emery AE (2002) The muscular dystrophies. Lancet 359(9307):687–695. doi:10.1016/S0140-6736(02)07815-7
3. Mazzone E, Vasco G, Sormani MP, Torrente Y, Berardinelli A, Messina S, D'Amico A, Doglio L, Politano L, Cavallaro F, Frosini S, Bello L, Bonfiglio S, Zucchini E, De Sanctis R, Scutifero M, Bianco F, Rossi F, Motta MC, Sacco A, Donati MA, Mongini T, Pini A, Battini R, Pegoraro E, Pane M, Gasperini S, Previtali S, Napolitano S, Martinelli D, Bruno C, Vita G, Comi G, Bertini E, Mercuri E (2011) Functional changes in Duchenne muscular dystrophy: a 12-month longitudinal cohort study. Neurology 77(3):250–256. doi:10.1212/WNL.0b013e318225ab2e
4. Vuillerot C, Girardot F, Payan C, Fermanian J, Iwaz J, De Lattre C, Berard C (2010) Monitoring changes and predicting loss of ambulation in Duchenne muscular dystrophy with the motor function measure. Dev Med Child Neurol 52(1):60–65. doi:10.1111/j.1469-8749.2009.03316.x

5. Fischmann A, Gloor M, Fasler S, Haas T, Rodoni Wetzel R, Bieri O, Wetzel S, Heinimann K, Scheffler K, Fischer D (2011) Muscular involvement assessed by MRI correlates to motor function measurement values in oculopharyngeal muscular dystrophy. J Neurol 258(7):1333–1340. doi:10.1007/s00415-011-5937-9
6. Sinclair CD, Morrow JM, Yousry TA, Reilly MM, Hanna MG, Golay X, Thornton JS (2010) Inter-scan reproducibility of quantitative neuromuscular MRI. Neuromuscul Disord 20:S28
7. Fischmann A, Hafner P, Fasler S, Gloor M, Bieri O, Studler U, Fischer D (2012) Quantitative MRI can detect subclinical disease progression in muscular dystrophy. J Neurol 259(8):1648–1654. doi:10.1007/s00415-011-6393-2
8. Hogrel JY, Wary C, Moraux A, Azzabou N, Decostre V, Ollivier G, Canal A, Lilien C, Ledoux I, Annoussamy M, Reguiba N, Gidaro T, Le Moing AG, Cardas R, Voit T, Carlier PG, Servais L (2016) Longitudinal functional and NMR assessment of upper limbs in Duchenne muscular dystrophy. Neurology 86(11):1022–1030. doi:10.1212/WNL.0000000000002464
9. Morrow JM, Sinclair CD, Fischmann A, Machado PM, Reilly MM, Yousry TA, Thornton JS, Hanna MG (2015) MRI biomarker assessment of neuromuscular disease progression: a prospective observational cohort study. Lancet Neurol 15(1):65–77. doi:10.1016/S1474-4422(15)00242-2
10. Willcocks RJ, Rooney WD, Triplett WT, Forbes SC, Lott DJ, Senesac CR, Daniels MJ, Wang DJ, Harrington AT, Tennekoon GI, Russman BS, Finanger EL, Byrne BJ, Finkel RS, Walter GA, Sweeney HL, Vandenborne K (2016) Multicenter prospective longitudinal study of magnetic resonance biomarkers in a large Duchenne muscular dystrophy cohort. Ann Neurol 79(4):535–547. doi:10.1002/ana.24599
11. Willis TA, Hollingsworth KG, Coombs A, Sveen M-L, Andersen S, Stojkovic T, Eagle M, Mayhew A, De Sousa PL, Dewar L, Morrow J, Sinclair CD, Thornton JS, Bushby K, Lochmuller H, Hanna M, Hogrel J-Y, Carlier PG, Vissing J, Straub V (2013) Quantitative muscle MRI as an assessment tool for monitoring disease progression in LGMD2I: a multicentre longitudinal study. PLoS One 8(8):e70993. doi:10.1371/journal.pone.0070993
12. Wokke BH, Bos C, Reijnierse M, van Rijswijk CS, Eggers H, Webb A, Verschuuren JJ, Kan HE (2013) Comparison of Dixon and T1-weighted MR methods to assess the degree of fat infiltration in Duchenne muscular dystrophy patients. J Magn Reson Imaging 38(3):619–624. doi:10.1002/jmri.23998
13. Gloor M, Fasler S, Fischmann A, Haas T, Bieri O, Heinimann K, Wetzel SG, Scheffler K, Fischer D (2011) Quantification of fat infiltration in oculopharyngeal muscular dystrophy: comparison of three MR imaging methods. J Magn Reson Imaging 33(1):203–210. doi:10.1002/jmri.22431
14. Hollingsworth KG, Garrood P, Eagle M, Bushby K, Straub V (2013) Magnetic resonance imaging in Duchenne muscular dystrophy: longitudinal assessment of natural history over 18 months. Muscle Nerve 48(4):586–588. doi:10.1002/mus.23879
15. Hu HH, Boernert P, Hernando D, Kellman P, Ma J, Reeder S, Sirlin C (2012) ISMRM workshop on fat–water separation: insights, applications and progress in MRI. Magn Reson Med 68(2):378–388. doi:10.1002/mrm.24369
16. Dixon WT (1984) Simple proton spectroscopic imaging. Radiology 153(1):189–194. doi:10.1148/radiology.153.1.6089263
17. Glover GH, Schneider E (1991) Three-point Dixon technique for true water/fat decomposition with B0 inhomogeneity correction. Magn Reson Med 18(2):371–383
18. Reeder SB, Pineda AR, Wen Z, Shimakawa A, Yu H, Brittain JH, Gold GE, Beaulieu CH, Pelc NJ (2005) Iterative decomposition of water and fat with echo asymmetry and least-squares estimation (IDEAL): application with fast spin-echo imaging. Magn Reson Med 54(3):636–644. doi:10.1002/mrm.20624
19. Hu HH, Li Y, Nagy TR, Goran MI, Nayak KS (2011) Quantification of absolute fat mass by magnetic resonance imaging: a validation study against chemical analysis. Int J Body Compos Res 9(3):111–122
20. Reeder SB, Hu HH, Sirlin CB (2012) Proton density fat-fraction: a standardized MR-based biomarker of tissue fat concentration. J Magn Reson Imaging 36(5):1011–1014. doi:10.1002/jmri.23741
21. Reeder SB, Wen Z, Yu H, Pineda AR, Gold GE, Markl M, Pelc NJ (2004) Multicoil Dixon chemical species separation with an iterative least-squares estimation method. Magn Reson Med 51(1):35–45. doi:10.1002/mrm.10675
22. Eggers H, Bornert P (2014) Chemical shift encoding-based water–fat separation methods. J Magn Reson Imaging 40(2):251–268. doi:10.1002/jmri.24568
23. Janiczek RL, Gambarota G, Sinclair CD, Yousry TA, Thornton JS, Golay X, Newbould RD (2011) Simultaneous T(2) and lipid quantitation using IDEAL-CPMG. Magn Reson Med 66(5):1293–1302. doi:10.1002/mrm.22916
24. Mankodi A, Bishop CA, Auh S, Newbould RD, Fischbeck KH, Janiczek RL (2016) Quantifying disease activity in fatty-infiltrated skeletal muscle by IDEAL-CPMG in Duchenne muscular dystrophy. Neuromuscul Disord 26(10):650–658. doi:10.1016/j.nmd.2016.07.013
25. Sinclair CD, Morrow JM, Janiczek RL, Evans MR, Rawah E, Shah S, Hanna MG, Reilly MM, Yousry TA, Thornton JS (2016) Stability and sensitivity of water T2 obtained with IDEAL-CPMG in healthy and fat–infiltrated skeletal muscle. NMR Biomed 29(12):1800–1812. doi:10.1002/nbm.3654
26. Boesch C (2007) Musculoskeletal spectroscopy. J Magn Reson Imaging 25(2):321–338. doi:10.1002/jmri.20806
27. Bottomley PA, Lee Y, Weiss RG (1997) Total creatine in muscle: imaging and quantification with proton MR spectroscopy. Radiology 204(2):403–410. doi:10.1148/radiology.204.2.9240527
28. Cullen CH, Ray GJ, Szabo CM (2013) A comparison of quantitative nuclear magnetic resonance methods: internal, external, and electronic referencing. Magn Reson Chem 51(11):705–713. doi:10.1002/mrc.4004
29. Reeder SB, Bice EK, Yu H, Hernando D, Pineda AR (2012) On the performance of T2* correction methods for quantification of hepatic fat content. Magn Reson Med 67(2):389–404. doi:10.1002/mrm.23016
30. Reeder SB, Cruite I, Hamilton G, Sirlin CB (2011) Quantitative assessment of liver fat with magnetic resonance imaging and spectroscopy. J Magn Reson Imaging 34(4):729–749. doi:10.1002/jmri.22580
31. Reeder SB, Robson PM, Yu H, Shimakawa A, Hines CD, McKenzie CA, Brittain JH (2009) Quantification of hepatic steatosis with MRI: the effects of accurate fat spectral modeling. J Magn Reson Imaging 29(6):1332–1339. doi:10.1002/jmri.21751
32. Mosconi E, Sima DM, Osorio Garcia MI, Fontanella M, Fiorini S, Van Huffel S, Marzola P (2014) Different quantification algorithms may lead to different results: a comparison using proton MRS lipid signals. NMR Biomed 27(4):431–443. doi:10.1002/nbm.3079
33. Kirchner T, Fillmer A, Tsao J, Pruessmann KP, Henning A (2015) Reduction of voxel bleeding in highly accelerated parallel (1) H MRSI by direct control of the spatial response function. Magn Reson Med 73(2):469–480. doi:10.1002/mrm.25185
34. Wilson NE, Burns BL, Iqbal Z, Thomas MA (2015) Correlated spectroscopic imaging of calf muscle in three spatial dimensions using group sparse reconstruction of undersampled single and multichannel data. Magn Reson Med 74(5):1199–1208. doi:10.1002/mrm.25988

35. Arpan I, Willcocks RJ, Forbes SC, Finkel RS, Lott DJ, Rooney WD, Triplett WT, Senesac CR, Daniels MJ, Byrne BJ, Finanger EL, Russman BS, Wang DJ, Tennekoon GI, Walter GA, Sweeney HL, Vandenborne K (2014) Examination of effects of corticosteroids on skeletal muscles of boys with DMD using MRI and MRS. Neurology 83(11):974–980. doi:10.1212/WNL.0000000000000775
36. Forbes SC, Walter GA, Rooney WD, Wang DJ, Devos S, Pollaro J, Triplett W, Lott DJ, Willcocks RJ, Senesac C, Daniels MJ, Byrne BJ, Russman B, Finkel RS, Meyer JS, Sweeney HL, Vandenborne K (2013) Skeletal muscles of ambulant children with Duchenne muscular dystrophy: validation of multicenter study of evaluation with MR imaging and MR spectroscopy. Radiology 269(1):198–207. doi:10.1148/radiol.13121948
37. Forbes SC, Willcocks RJ, Triplett WT, Rooney WD, Lott DJ, Wang DJ, Pollaro J, Senesac CR, Daniels MJ, Finkel RS, Russman BS, Byrne BJ, Finanger EL, Tennekoon GI, Walter GA, Sweeney HL, Vandenborne K (2014) Magnetic resonance imaging and spectroscopy assessment of lower extremity skeletal muscles in boys with Duchenne muscular dystrophy: a multicenter cross sectional study. PLoS One 9(9):e106435. doi:10.1371/journal.pone.0106435
38. Triplett WT, Baligand C, Forbes SC, Willcocks RJ, Lott DJ, Devos S, Pollaro J, Rooney WD, Sweeney HL, Bönnemann CG, Wang DJ, Vandenborne K, Walter GA (2014) Chemical shift-based MRI to measure fat fractions in dystrophic skeletal muscle. Magn Reson Med 72(1):8–19
39. Wokke BH, van den Bergen JC, Versluis MJ, Niks EH, Milles J, Webb AG, van Zwet EW, Aartsma-Rus A, Verschuuren JJ, Kan HE (2014) Quantitative MRI and strength measurements in the assessment of muscle quality in Duchenne muscular dystrophy. Neuromuscul Disord 24(5):409–416. doi:10.1016/j.nmd.2014.01.015
40. Willis TA, Hollingsworth KG, Coombs A, Sveen ML, Andersen S, Stojkovic T, Eagle M, Mayhew A, de Sousa PL, Dewar L, Morrow JM, Sinclair CD, Thornton JS, Bushby K, Lochmuller H, Hanna MG, Hogrel JY, Carlier PG, Vissing J, Straub V (2014) Quantitative magnetic resonance imaging in limb-girdle muscular dystrophy 2I: a multinational cross-sectional study. PLoS One 9(2):e90377. doi:10.1371/journal.pone.0090377
41. Lokken N, Hedermann G, Thomsen C, Vissing J (2016) Contractile properties are disrupted in Becker muscular dystrophy, but not in limb girdle type 2I. Ann Neurol 80(3):466–471. doi:10.1002/ana.24743
42. Carlier PG, Azzabou N, de Sousa PL, Hicks A, Boisserie JM, Amadon A, Carlier RY, Wary C, Orlikowski D, Laforet P (2015) Skeletal muscle quantitative nuclear magnetic resonance imaging follow-up of adult Pompe patients. J Inherit Metab Dis 38(3):565–572. doi:10.1007/s10545-015-9825-9
43. Loughran T, Higgins DM, McCallum M, Coombs A, Straub V, Hollingsworth KG (2015) Improving highly accelerated fat fraction measurements for clinical trials in muscular dystrophy: origin and quantitative effect of R2* changes. Radiology 275(2):570–578. doi:10.1148/radiol.14141191
44. Ricotti V, Evans MR, Sinclair CD, Butler JW, Ridout DA, Hogrel JY, Emira A, Morrow JM, Reilly MM, Hanna MG, Janiczek RL, Matthews PM, Yousry TA, Muntoni F, Thornton JS (2016) Upper limb evaluation in Duchenne muscular dystrophy: fat–water quantification by MRI, muscle force and function define endpoints for clinical trials. PLoS One 11(9):e0162542. doi:10.1371/journal.pone.0162542
45. Hollingsworth KG, Higgins DM, McCallum M, Ward L, Coombs A, Straub V (2014) Investigating the quantitative fidelity of prospectively undersampled chemical shift imaging in muscular dystrophy with compressed sensing and parallel imaging reconstruction. Magn Reson Med 72(6):1610–1619. doi:10.1002/mrm.25072
46. Hooijmans MT, Niks EH, Burakiewicz J, Verschuuren JJ, Webb AG, Kan HE (2017) Elevated phosphodiester and T2 levels can be measured in the absence of fat infiltration in Duchenne muscular dystrophy patients. NMR Biomed. doi:10.1002/nbm.3667
47. Hollingsworth KG, de Sousa PL, Straub V, Carlier PG (2012) Towards harmonization of protocols for MRI outcome measures in skeletal muscle studies: consensus recommendations from two TREAT-NMD NMR workshops, 2 May 2010, Stockholm, Sweden, 1–2 October 2009, Paris. France. Neuromuscul Disord 22(Suppl 2):S54–S67. doi:10.1016/j.nmd.2012.06.005
48. Bernard CP, Liney GP, Manton DJ, Turnbull LW, Langton CM (2008) Comparison of fat quantification methods: a phantom study at 3.0T. J Magn Reson Imaging 27(1):192–197. doi:10.1002/jmri.21201
49. Hines CD, Frydrychowicz A, Hamilton G, Tudorascu DL, Vigen KK, Yu H, McKenzie CA, Sirlin CB, Brittain JH, Reeder SB (2011) T1 independent, T2* corrected chemical shift based fat–water separation with multi-peak fat spectral modeling is an accurate and precise measure of hepatic steatosis. J Magn Reson Imaging 33(4):873–881. doi:10.1002/jmri.22514
50. Hines CD, Yu H, Shimakawa A, McKenzie CA, Brittain JH, Reeder SB (2009) T1 independent, T2* corrected MRI with accurate spectral modeling for quantification of fat: validation in a fat–water-SPIO phantom. J Magn Reson Imaging 30(5):1215–1222. doi:10.1002/jmri.21957
51. Janssen BH, Voet NB, Nabuurs CI, Kan HE, de Rooy JW, Geurts AC, Padberg GW, van Engelen BG, Heerschap A (2014) Distinct disease phases in muscles of facioscapulohumeral dystrophy patients identified by MR detected fat infiltration. PLoS One 9(1):e85416. doi:10.1371/journal.pone.0085416
52. Willcocks RJ, Triplett WT, Forbes SC, Arora H, Senesac CR, Lott DJ, Nicholson TR, Rooney WD, Walter GA, Vandenborne K (2017) Magnetic resonance imaging of the proximal upper extremity musculature in boys with Duchenne muscular dystrophy. J Neurol 264(1):64–71. doi:10.1007/s00415-016-8311-0
53. Machann J, Thamer C, Schnoedt B, Haap M, Haring HU, Claussen CD, Stumvoll M, Fritsche A, Schick F (2005) Standardized assessment of whole body adipose tissue topography by MRI. J Magn Reson Imaging 21(4):455–462. doi:10.1002/jmri.20292
54. Wary C, Azzabou N, Giraudeau C, Le Louer J, Montus M, Voit T, Servais L, Carlier P (2015) Quantitative NMRI and NMRS identify augmented disease progression after loss of ambulation in forearms of boys with Duchenne muscular dystrophy. NMR Biomed 28(9):1150–1162. doi:10.1002/nbm.3352
55. Sinclair CD, Morrow JM, Miranda MA, Davagnanam I, Cowley PC, Mehta H, Hanna MG, Koltzenburg M, Yousry TA, Reilly MM, Thornton JS (2012) Skeletal muscle MRI magnetisation transfer ratio reflects clinical severity in peripheral neuropathies. J Neurol Neurosurg Psychiatry 83(1):29–32. doi:10.1136/jnnp.2011.246116
56. Lareau-Trudel E, Le Troter A, Ghattas B, Pouget J, Attarian S, Bendahan D, Salort-Campana E (2015) Muscle quantitative MR imaging and clustering analysis in patients with facioscapulohumeral muscular dystrophy type 1. PLoS One 10(7):e0132717. doi:10.1371/journal.pone.0132717
57. Makrogiannis S, Serai S, Fishbein KW, Schreiber C, Ferrucci L, Spencer RG (2012) Automated quantification of muscle and fat in the thigh from water-, fat-, and nonsuppressed MR images. J Magn Reson Imaging 35(5):1152–1161. doi:10.1002/jmri.22842
58. Positano V, Christiansen T, Santarelli MF, Ringgaard S, Landini L, Gastaldelli A (2009) Accurate segmentation of subcutaneous and intermuscular adipose tissue from MR images of the thigh. J Magn Reson Imaging 29(3):677–684. doi:10.1002/jmri.21699
59. Valentinitsch A, Karampinos DC, Alizai H, Subburaj K, Kumar D, Link TM, Majumdar S (2013) Automated unsupervised multi-

parametric classification of adipose tissue depots in skeletal muscle. J Magn Reson Imaging 37(4):917–927. doi:10.1002/jmri.23884
60. Baudin PY, Azzabou N, Carlier PG, Paragios N (2012) Prior knowledge, random walks and human skeletal muscle segmentation. Med Image Comput Comput Assist Interv 15(Pt 1):569–576
61. Commean PK, Tuttle LJ, Hastings MK, Strube MJ, Mueller MJ (2011) Magnetic resonance imaging measurement reproducibility for calf muscle and adipose tissue volume. J Magn Reson Imaging 34(6):1285–1294. doi:10.1002/jmri.22791
62. Yu H, Shimakawa A, McKenzie CA, Brodsky E, Brittain JH, Reeder SB (2008) Multiecho water–fat separation and simultaneous R2* estimation with multifrequency fat spectrum modeling. Magn Reson Med 60(5):1122–1134. doi:10.1002/mrm.21737
63. Mann LW, Higgins DM, Peters CN, Cassidy S, Hodson KK, Coombs A, Taylor R, Hollingsworth KG (2016) Accelerating MR imaging liver steatosis measurement using combined compressed sensing and parallel imaging: a quantitative evaluation. Radiology 278(1):247–256. doi:10.1148/radiol.2015150320
64. Liu C-Y, McKenzie CA, Yu H, Brittain JH, Reeder SB (2007) Fat quantification with IDEAL gradient echo imaging: correction of bias from T-1 and noise. Magn Reson Med 58(2):354–364. doi:10.1002/mrm.21301
65. Hu HH, Nayak KS (2010) Change in the proton T1 of fat and water in mixture. Magn Reson Med 63(2):494–501. doi:10.1002/mrm.22205
66. Yu H, McKenzie CA, Shimakawa A, Vu AT, Brau AC, Beatty PJ, Pineda AR, Brittain JH, Reeder SB (2007) Multiecho reconstruction for simultaneous water–fat decomposition and T2* estimation. J Magn Reson Imaging 26(4):1153–1161. doi:10.1002/jmri.21090
67. Hamilton G, Yokoo T, Bydder M, Cruite I, Schroeder ME, Sirlin CB, Middleton MS (2011) In vivo characterization of the liver fat H-1 MR spectrum. NMR Biomed 24(7):784–790. doi:10.1002/nbm.1622
68. Ren J, Dimitrov I, Sherry AD, Malloy CR (2008) Composition of adipose tissue and marrow fat in humans by 1H NMR at 7 Tesla. J Lipid Res 49(9):2055–2062. doi:10.1194/jlr.D800010-JLR200
69. Hernando D, Karampinos DC, King KF, Haldar JP, Majumdar S, Georgiadis JG, Liang ZP (2011) Removal of olefinic fat chemical shift artifact in diffusion MRI. Magn Reson Med 65(3):692–701. doi:10.1002/mrm.22670
70. Pineda AR, Reeder SB, Wen Z, Pelc NJ (2005) Cramer-Rao bounds for three-point decomposition of water and fat. Magn Reson Med 54(3):625–635. doi:10.1002/mrm.20623
71. Fischmann A, Hafner P, Gloor M, Schmid M, Klein A, Pohlman U, Waltz T, Gonzalez R, Haas T, Bieri O, Fischer D (2013) Quantitative MRI and loss of free ambulation in Duchenne muscular dystrophy. J Neurol 260(4):969–974. doi:10.1007/s00415-012-6733-x
72. Gaeta M, Messina S, Mileto A, Vita GL, Ascenti G, Vinci S, Bottari A, Vita G, Settineri N, Bruschetta D, Racchiusa S, Minutoli F (2012) Muscle fat-fraction and mapping in Duchenne muscular dystrophy: evaluation of disease distribution and correlation with clinical assessments. Preliminary experience. Skeletal Radiol 41(8):955–961. doi:10.1007/s00256-011-1301-5
73. Hooijmans MT, Niks EH, Burakiewicz J, Anastasopoulos C, van den Berg SI, van Zwet E, Webb AG, Verschuuren JJ, Kan HE (2017) Non-uniform muscle fat replacement along the proximodistal axis in Duchenne muscular dystrophy. Neuromuscul Disord 27(5):458–464. doi:10.1016/j.nmd.2017.02.009
74. Horvath JJ, Austin SL, Case LE, Greene KB, Jones HN, Soher BJ, Kishnani PS, Bashir MR (2015) Correlation between quantitative whole-body muscle magnetic resonance imaging and clinical muscle weakness in Pompe disease. Muscle Nerve 51(5):722–730. doi:10.1002/mus.24437
75. van den Bergen JC, Wokke BH, Janson AA, van Duinen SG, Hulsker MA, Ginjaar HB, van Deutekom JC, Aartsma-Rus A, Kan HE, Verschuuren JJ (2014) Dystrophin levels and clinical severity in Becker muscular dystrophy patients. J Neurol Neurosurg Psychiatry 85(7):747–753. doi:10.1136/jnnp-2013-306350
76. Wokke BH, Hooijmans MT, van den Bergen JC, Webb AG, Verschuuren JJ, Kan HE (2014) Muscle MRS detects elevated PDE/ATP ratios prior to fatty infiltration in Becker muscular dystrophy. NMR Biomed 27(11):1371–1377. doi:10.1002/nbm.3199
77. Wren TA, Bluml S, Tseng-Ong L, Gilsanz V (2008) Three-point technique of fat quantification of muscle tissue as a marker of disease progression in Duchenne muscular dystrophy: preliminary study. AJR Am J Roentgenol 190(1):W8–12. doi:10.2214/AJR.07.2732
78. Andersen G, Dahlqvist JR, Vissing CR, Heje K, Thomsen C, Vissing J (2017) MRI as outcome measure in facioscapulohumeral muscular dystrophy: 1-year follow-up of 45 patients. J Neurol 264(3):438–447. doi:10.1007/s00415-016-8361-3
79. Bonati U, Hafner P, Schadelin S, Schmid M, Naduvilekoot Devasia A, Schroeder J, Zuesli S, Pohlman U, Neuhaus C, Klein A, Sinnreich M, Haas T, Gloor M, Bieri O, Fischmann A, Fischer D (2015) Quantitative muscle MRI: a powerful surrogate outcome measure in Duchenne muscular dystrophy. Neuromuscul Disord 25(9):679–685. doi:10.1016/j.nmd.2015.05.006
80. Bonati U, Schmid M, Hafner P, Haas T, Bieri O, Gloor M, Fischmann A, Fischer D (2015) Longitudinal 2-point Dixon muscle magnetic resonance imaging in Becker muscular dystrophy. Muscle Nerve 51(6):918–921. doi:10.1002/mus.24629
81. Bonati U, Holiga S, Hellbach N, Risterucci C, Bergauer T, Tang W, Hafner P, Thoeni A, Bieri O, Gerlach I, Marquet A, Khwaja O, Sambataro F, Bertolino A, Dukart J, Fischmann A, Fischer D, Czech C (2017) Longitudinal characterization of biomarkers for spinal muscular atrophy. Ann Clin Transl Neurol 4(5):292–304. doi:10.1002/acn3.406
82. Azzabou N, Loureiro de Sousa P, Caldas E, Carlier PG (2015) Validation of a generic approach to muscle water T2 determination at 3T in fat-infiltrated skeletal muscle. J Magn Reson Imaging 41(3):645–653. doi:10.1002/jmri.24613
83. Hooijmans MT, Damon BM, Froeling M, Versluis MJ, Burakiewicz J, Verschuuren JJ, Niks EH, Webb AG, Kan HE (2015) Evaluation of skeletal muscle DTI in patients with Duchenne muscular dystrophy. NMR Biomed 28(11):1589–1597. doi:10.1002/nbm.3427
84. Marty B, Baudin PY, Reyngoudt H, Azzabou N, Araujo EC, Carlier PG, de Sousa PL (2016) Simultaneous muscle water T2 and fat fraction mapping using transverse relaxometry with stimulated echo compensation. NMR Biomed 29(4):431–443. doi:10.1002/nbm.3459
85. Ponrartana S, Ramos-Platt L, Wren TA, Hu HH, Perkins TG, Chia JM, Gilsanz V (2015) Effectiveness of diffusion tensor imaging in assessing disease severity in Duchenne muscular dystrophy: preliminary study. Pediatr Radiol 45(4):582–589. doi:10.1007/s00247-014-3187-6